Published in final edited form as:
Cell Metab. 2014 January 7; 19(1): 162–171. doi:10.1016/j.cmet.2013.11.017.

Local proliferation of macrophages contributes to obesity-associated adipose tissue inflammation

Shinya U. Amano[#1], **Jessica L. Cohen**[#1], **Pranitha Vangala**[1], **Michaela Tencerova**[1], **Sarah M. Nicoloro**[1], **Joseph C. Yawe**[1], **Yuefei Shen**[1], **Michael P. Czech**[1,*], and **Myriam Aouadi**[1,*]

[1]Program in Molecular Medicine, University of Massachusetts Medical School, Worcester, Massachusetts 01605, USA.

[#] These authors contributed equally to this work.

SUMMARY

Adipose tissue (AT) of obese mice and humans accumulates immune cells, which secrete cytokines that can promote insulin resistance. AT macrophages (ATMs) are thought to originate from bone marrow-derived monocytes, which infiltrate the tissue from the circulation. Here we show that a major fraction of macrophages unexpectedly undergo cell division locally within AT, as detected by Ki67 expression and 5-ethynyl-2′-deoxyuridine incorporation. Macrophages within the visceral AT (VAT), but not those in other tissues, including liver and spleen, displayed increased proliferation in obesity. Importantly, depletion of blood monocytes had no impact on ATM content, while their proliferation *in situ* continued. Treatment with monocyte chemotactic protein 1 (MCP-1) induced macrophage cell division in AT explants, while MCP-1 deficiency *in vivo* decreased ATM proliferation. These results reveal that proliferation *in situ* driven by MCP-1 is an important process by which macrophages accumulate in the VAT in obesity, in addition to blood monocyte recruitment.

INTRODUCTION

Obesity can induce an insulin-resistant state in adipose tissue (AT), liver, and skeletal muscle and is a strong risk factor for the development of type 2 diabetes (T2D) (Guilherme et al., 2008; Olefsky and Glass, 2010). It is increasingly appreciated that accumulation of macrophages and other immune cell types in AT correlates with a chronic inflammatory state that ultimately impairs adipocyte function and may contribute to the development of insulin resistance (Aouadi et al., 2013;Olefsky and Glass, 2010; Weisberg et al., 2003).

The origin of macrophages in AT has previously been attributed to recruitment of blood monocytes into AT based on one study using irradiation followed by bone marrow transplant (Weisberg et al., 2003). Therefore, strategies to decrease ATM accumulation have been particularly focused on decreasing macrophage migration into the AT by depleting blood monocytes or genes encoding chemokines that attract macrophages into the AT (Feng et al., 2011; Kanda et al., 2006; Nomiyama et al., 2007; Weisberg et al., 2006). However,

[*]Correspondence: michael.czech@umassmed.edu; myriam.aouadi@umassmed.edu.

The authors report that they have no conflicts of interest.

studies using these approaches do not address whether migration is the only process contributing to macrophage accumulation in the AT. The present study was designed to determine whether significant macrophage cell division also occurs within VAT in mice.

RESULTS-DISCUSSION

Macrophages proliferate locally within the adipose tissue

To confirm macrophage accumulation in AT of obese mice, we used 8 to 12-week old genetically obese (*ob*/*ob*) male mice and their lean control wild-type (WT) littermates. The stromal-vascular fraction (SVF) from VAT and subcutaneous AT (SAT), was stained with antibodies against macrophage markers, F4/80 and CD11b, an eosinophil marker, Siglec-f, and a neutrophil marker, Gr-1 and analyzed by flow cytometry. The macrophage population in the AT was defined as $F4/80^{+}/CD11b^{+}/Siglec\text{-}f^{-}/Gr\text{-}1^{-}$ (for the complete gating scheme see Figure S1A). Consistent with published studies (Weisberg et al., 2003; Xu et al., 2003), macrophage content was significantly increased in the VAT of *ob*/*ob* compared to WT mice (*ob/ob* 959 ± 69 $\times 10^3$ *vs.* WT 140 ± 35 $\times 10^3$ macrophages/g of VAT, p<0.001 and Figure 1A-B). The number as well as the percentage of macrophages was also increased in the SAT of *ob/ob* compared to WT mice but to a lower extent than in VAT (*ob/ob* 192 ± 31 $\times 10^3$ *vs.* WT 109 ± 12 $\times 10^3$ macrophages/g of SAT, p=0.04 and Figure S1B). These results confirmed that macrophages accumulate mostly in the VAT in mice in response to obesity.

To test whether ATM proliferation increases in the inflammatory setting of obesity, SVF cells from WT and *ob/ob* mice were stained with an antibody against the proliferation marker Ki67, which is a protein expressed during all active phases of the cell cycle (Scholzen and Gerdes, 2000). Ki67 signal was detected in approximately 2.3% of ATMs from VAT of lean WT mice, and in 10% of ATMs of *ob*/*ob* mice (*ob*/*ob* 94 ± 7 $\times 10^3$ *vs.* WT 7.6 ± 3.2 $\times 10^3$ macrophages/g of VAT, p<0.001 and Figure 1C-D). The percentage of $Ki67^{+}$ macrophages was also increased in the SAT from *ob/ob* compared to WT mice (Figure S1C). However, the number of $Ki67^{+}$ macrophages was lower in SAT compared to VAT in *ob/ob* mice (SAT 20.0 ± 3.3 $\times 10^3$ *vs.* VAT 94 ± 7 $\times 10^3$ macrophages/g, p<0.001). This suggests that macrophages preferentially accumulate and proliferate in the VAT of obese mice. Consistent with the flow cytometry analysis, immunofluorescence microscopy on SVF cells and VAT of *ob*/*ob* mice showed macrophages expressing Ki67 in their nuclei (Figure 1E-F). Interestingly most of the Ki67 staining was observed in macrophages in a region of the VAT rich in macrophages termed crown-like structures (CLS) (Figure 1F).

Similar to genetically induced obesity, diet-induced obesity increased macrophage content in the AT (Figure 1G-H). ATM number was significantly higher in SVF of VAT in mice fed a high fat diet (HFD) compared to normal chow diet (ND) (HFD 1,045 ± 131 $\times 10^3$ *vs.* ND 140 ± 35 $\times 10^3$ macrophages/g of VAT, p<0.001). More importantly, in mice fed a HFD, 17% of ATMs were $Ki67^{+}$ compared to 3% in mice fed a ND (HFD 183 ± 21 $\times 10^3$ *vs.* ND 7.6 ± 3.2 $\times 10^3$ macrophages/g of VAT, p<0.001) (Figure 1 I-J). Consistent with published data (Bourlier et al., 2008) and as suggested by gene expression profile analysis of human ATMs (Mayi et al., 2012), flow cytometry analysis of SVF stained with Ki67 antibody showed that approximately 8% of ATMs proliferate in AT (7.7 ± 1.9 %; n=5; Figure 1K). Taken together, these results show by both flow cytometry and microscopic analysis that macrophages express the proliferation marker Ki67 in the AT in mice and humans and to higher degree in response to obesity in mice caused by either genetic mutation or a diet high in fat.

We next tested whether fasting-induced weight loss also regulates ATM proliferation. After a 24-hour fast mice lost an average of 5 percent body weight (data not shown). While the percentage of ATM was slightly decreased, the number of ATM was significantly decreased

in VAT of mice fed a HFD after a 24-hour fast (Figure 1L-M). Although this could be explained by a concomitant decrease in non-macrophage cells, it has been shown that fasting induces the formation of lipid-laden macrophages attached to the adipocyte fraction (Kosteli et al., 2010). Interestingly, ATM proliferation was significantly decreased after a 24-hour fast, suggesting a correlation between macrophage content and proliferation in the AT (Figure 1N).

It is interesting to note that fasting had no effect on proliferation of F4/80−/CD11b− cells, which could include cell types that have been shown to proliferate *in situ* in the AT, including T cells (Morris et al., 2013a) and adipocyte progenitors (Lee et al., 2012) (Figure 1O). Taken together, these results suggest that changes occurring during AT mass regulation selectively affect proliferation of specific cell types in AT, including macrophages.

Obesity stimulates macrophage proliferation specifically in the adipose tissue

To test whether macrophage proliferation increases with obesity in tissues other than AT, we analyzed the proliferation rate of macrophages in spleen and liver following a 3-hour pulse of the nucleoside analog to thymidine, EdU, which is incorporated into DNA only during the S-phase. Approximately 1% of ATMs in lean mice and about 4.5% of the macrophages in the obese mice were in S-phase during the pulse of EdU (Figure 2A), confirming that obesity increases ATM proliferation. In contrast, less than 2% of all cells, including macrophages, were EdU^+ in spleen and liver, and there was no difference in EdU^+ cells between lean and obese mice in these tissues (Figure 2B-C). This striking specificity for increased macrophage proliferation in AT in obesity implies that the AT micro-environment is important for macrophage proliferation.

Monocytes failed to display detectable EdU incorporation within the 3-hour pulse in lean or obese mice, suggesting that EdU^+ macrophages observed in the AT are not recently recruited blood monocytes (Figure 2D). Importantly, obesity did not affect the EdU incorporation rate in spleen, liver or blood macrophages (Figure 2E). Interestingly, macrophage content increased with obesity in AT (Figure 1A), while there was no change or a slight decrease in spleen or liver in *ob*/*ob* mice compared to WT mice (Figure 2 F). This further confirms a correlation between macrophage accumulation and proliferation in tissues and suggests that AT provides a unique environment facilitating macrophage proliferation.

In order to study the selective effect of obesity on immune cell proliferation, we analyzed Ki67 staining in eosinophils and neutrophils, whose content in the AT has been shown to be regulated by obesity (Talukdar et al., 2012; Wu et al., 2011). Consistent with a prior report (Wu et al., 2011), we found that eosinophil content relative to macrophages in the AT decreased with obesity (Figure S2A-C). Neutrophil content in AT was not significantly different between WT and *ob*/*ob* mice (Figure S2D-F). While both eosinophils and neutrophils have been shown to have some proliferative capacity outside of the bone marrow (Bjornson et al., 1985; Yang and Renzi, 1993), we failed to detect any EdU incorporation into these cells within AT (Figure S2C and F). Our results suggest that obesity does not stimulate proliferation of all cells in the AT, but selectively stimulates proliferation of specific cell types including macrophages.

Macrophage proliferation contributes to adipose tissue inflammation independently of monocyte recruitment

To further ensure that the proliferating macrophages in the AT were not recently recruited EdU^+ blood monocytes, we next studied the capacity of ATMs to proliferate *ex vivo*. SVF cells isolated from VAT of lean and obese mice were plated and treated with EdU for three hours. Approximately 0.3% of the ATMs from lean mice were EdU^+, while greater than 2%

were positive in macrophages from obese mice (Figure S3A-B). These results suggest that ATMs have the inherent capacity to proliferate *ex vivo*, independently of blood monocyte recruitment. To test this hypothesis, we depleted blood monocytes in *ob/ob* mice by intravenous (i.v.) injection of clodronate-loaded liposomes (Clod-Lipo), which induce apoptosis once ingested by monocytes (Feng et al., 2011). Consistent with published studies, Clod-Lipo i.v. injection depleted about 80% of blood monocytes 16 hours after injection compared to a PBS-liposome (PBS-Lipo) injection (Figure 3A-B). We then injected *ob/ob* mice every 16 hours with Clod-Lipo to maintain blood monocyte depletion and measured macrophage content in the VAT. Unexpectedly, ATM absolute number (48 hours, PBS-lipo 3.78 ± 0.37 *vs.* Clod-Lipo 3.88 ± 0.35; 96 hours, PBS-lipo 4.54 ± 0.60 *vs.* Clod-Lipo 3.36 ± 0.11 $\times 10^6$ cells/g of VAT) and ATM percentage in the SVF were unchanged with Clod-Lipo treatment even after prolonged blood monocyte depletion (Figure 3C). These data raised the possibility that the increase in macrophages that occurs during obesity was largely the result of proliferation of the resident population. Therefore, *ob/ob* mice were given EdU in drinking water during monocyte depletion as depicted in diagram in Figure 3D. Eighty hours after EdU exposure, about half of the macrophages in the AT of *ob/ob* mice injected with PBS-Lipo had incorporated EdU (Figure 3E-F). Importantly, depletion of blood monocytes had no effect on macrophage proliferation as observed by the EdU incorporation in the VAT of *ob/ob* mice injected with Clod-Lipo (Figure 3E-F). Interestingly, no difference in EdU incorporation was observed in macrophages in SAT of *ob/ob* compared to WT mice after 80 hours of EdU exposure (Figure 3G). This suggested that macrophage proliferation plays a major role in VAT macrophage expansion in obesity independently of monocyte recruitment. However, recently recruited macrophages may also proliferate in AT of obese mice since a recent study showed that 5% of labeled blood monocytes, transferred from donor into recipient mice, express Ki67 in the host AT two days after transfer (Oh et al., 2011).

While macrophage sub-populations in the AT may have overlapping marker expression profiles, it is generally thought that CD11c expression is characteristic of pro-inflammatory macrophage subtypes (Lumeng et al., 2008). Therefore, we analyzed the rate of proliferation of pro- ($CD11c^+$) and anti- ($CD11c^-$) inflammatory macrophages (Figure S3C). We failed to observe any difference in the rate of proliferation of macrophage population subtypes. This suggests that obesity increases macrophage proliferation rate independently of their inflammatory state. It has been previously shown that CLS density is higher in VAT compared to the SAT in obese mice (Murano et al., 2008). Interestingly, microscopic analysis of VAT sections showed that EdU was mostly incorporated in macrophages in CLS (Figure 3H). All together these results suggest that ATM proliferation occurs at a high rate in the VAT where macrophage content and CLS density are greatly increased by obesity.

MCP-1 stimulates adipose tissue macrophage proliferation

To investigate the mechanism by which obesity stimulates macrophage proliferation selectively in the AT, we measured in AT and liver of lean (ND and WT) and obese (HFD and *ob/ob*) mice the expression of multiple cytokines known to play a role in macrophage proliferation and infiltration. These included interleukin-4 (IL-4) (Jenkins et al., 2011), macrophage colony-stimulating factor (M-CSF) (Hashimoto et al., 2013), osteopontin (OPN) (Nomiyama et al., 2007) and monocyte chemotactic protein also referred to as chemokine (C-C motif) ligand 2 (CCL2/MCP-1) (Kanda et al., 2006; Weisberg et al., 2006) (Figure 4A-D and Figure S4A-D). Only OPN and MCP-1 expression was significantly increased with obesity (Figure 4A-D and Figure S4A-D). As described in Figures 1 and 2, macrophage proliferation was mainly increased in VAT in obese mice compared to lean, therefore we next measured the expression of OPN and MCP-1 in this fat depot compared to SAT and liver, where ATM proliferation is minimal (Figure 4E-F). Although OPN

expression was unchanged in SAT with obesity, it was significantly increased in liver (Figure 4E). In addition, OPN expression was similar in liver and VAT in mice fed a HFD (Figure 4E). In contrast, MCP-1 expression was significantly higher in VAT compared to liver and SAT in obese mice (Figure 4F). In addition, MCP-1 was the only cytokine that was decreased with fasting, consistent with a recent study (Asterholm et al., 2012) (Figure 4G and Figure S4E). This suggests a positive correlation between MCP-1 expression and macrophage proliferation in mice.

Based on the above analysis, the expression of MCP-1 in adipocytes and SVF from VAT of mice fed a HFD was measured. Although MCP-1 expression was high in both fractions, it was significantly higher in the adipocytes (Figure S4F). Interestingly the MCP-1 receptor, chemokine (C-C motif) receptor 2 (CCR2), has been shown to be mostly expressed in macrophages in CLS where most of proliferating ATMs were observed (Lumeng et al., 2008). These results suggest that MCP-1 released by adipocytes in CLS could stimulate proliferation of surrounding ATMs.

To test whether MCP-1 regulates ATM proliferation, mice lacking the *mcp-1* gene and their WT littermates were fed a HFD and ATM content and proliferation was measured in the VAT after 30 hours of EdU administration in drinking water (Figure 4H-K). HFD-induced obesity significantly increased ATM content, while fasting decreased the percentage of macrophages in the VAT (Figure 4H-I). Most importantly, we observed a significant decrease in the percentage and number of macrophages in the VAT from MCP-1 KO compared to WT (Figure 4H-I). RT-PCR analysis revealed that F4/80 and CD11b expression was decreased in the VAT of MCP-1 KO compared to WT mice fed a HFD, confirming the decreased ATM content (Figure S4G). In addition, MCP-1 deficiency was associated with a decrease in the total number of SVF cells (WTHFD,1836.78 ± 256.77 *vs.* MCP-1 KO, 287.96 ± 74.40), suggesting a general effect of MCP-1 on immune cell accumulation in AT as suggested in other tissues (Allavena et al., 1994; Jimenez et al., 2010). On the other hand, macrophages in the adipose tissue have been shown to play the role of antigen presenting cells able to induce T cell proliferation (Morris et al., 2013b), suggesting that the decreased ATM accumulation observed in MCP-1 KO mice could result in decreased T cell proliferation. Interestingly, fasting had no additional effect on ATM content in MCP-1 KO, suggesting that MCP-1 could be a major regulator of macrophage content in the VAT (Figure 4H-I). EdU staining analysis showed that the percentage and number of EdU^+ ATMs decreases with fasting and *mcp-1* deficiency, suggesting that the decrease in ATM content observed in MCP-1 KO mice could be due to a decreased rate of proliferation (Figure 4J-K). Interestingly, MCP-1 deficiency had no effect on the percentage of macrophages in liver and SAT, confirming the selective role of MCP-1 in the regulation of macrophage content in the VAT (Figure S4H).

Although MCP-1 has been shown to stimulate proliferation of multiple cell types (Hinojosa et al., 2011; Sager et al., 2010), it has been extensively described as a chemokine attracting macrophages from the blood to the AT in obese mice (Kanda et al., 2006; Weisberg et al., 2006). Thus, to test whether MCP-1 regulates ATM proliferation independently of macrophage recruitment, the monocyte content in the blood of MCP-1 KO and WT mice was analyzed (Figure 4L). We observed an increase in circulating monocytes in control mice with HFD compared to ND (Figure 4L), suggesting that monocyte recruitment contributes to macrophage accumulation in the AT. However, monocyte number in the blood remained the same in fed and fasted states in MCP-1 KO and WT mice, indicating that fasting-associated MCP-1 decrease or MCP-1 deficiency lowers ATM content mostly by decreasing proliferation (Figure 4L). To test this hypothesis, EdU incorporation in ATM was measured in VAT explants from *ob/ob* mice treated with MCP-1. Consistent with the hypothesis that MCP-1 regulates the accumulation of multiple cell types, treatment of explants with MCP-1

ex vivo increased the total number of SVCs (untreated, 1961.15 ± 788.00 *vs.* MCP1 (10 ng/ml), 4404.80 ± 353.66). Importantly, MCP-1 treatment significantly increased the number of ATMs and EdU incorporation (Figure 4M-N). Although proliferation may be regulated by multiple factors, MCP-1 plays a major role in regulating macrophage proliferation in the AT of obese mice independently of monocyte recruitment. However, these data do not exclude the contribution of monocyte recruitment and subsequent proliferation in the AT in obesity.

Next body weight, glucose tolerance and fasting glycaemia were measured in MCP-1 KO and WT mice fed a HFD to assess the metabolic consequences of a decreased ATM proliferation (Figure 4O-Q). The body weight of MCP-1 KO was slightly but not significantly higher than WT mice fed a HFD and both were significantly higher than WT mice fed a ND (Figure 4O). Surprisingly, although *mcp-1* deficiency led to a lower rate of macrophage proliferation in the AT and consequently a decreased ATM content, glucose intolerance was exacerbated in MCP-1 KO compared to WT mice (Figure 4P). Similarly, fasting blood glucose levels were significantly elevated in MCP-1 KO compared to WT mice (Figure 4Q). This result corroborated data from a previous study showing that MCP-1 KO mice fed a HFD are more glucose intolerant that their WT littermates (Inouye et al., 2007). However, the study by Inouye *et al*. showed that macrophage content is slightly increased in the VAT of MCP-1 KO compared to WT mice. One of the reasons for this discrepancy could be the gating scheme used to define macrophages in the AT. In our study macrophages were defined as $F4/80^{+}/CD11b^{+}/siglec\text{-}f^{-}/Gr1^{-}$ (see gating scheme in Figure S1) *vs.* $F4/80^{+}/CD11b^{+}$, which includes eosinophils and neutrophils, in the Inouye *et al*. study.

Taken together, these results show that a decreased ATM proliferation is associated with exacerbated glucose intolerance. While much of the relevant literature suggests macrophages in AT are inhibitory to adipose function (Olefsky and Glass, 2010), some data indicate a beneficial role, for example in increasing adipose lipid storage or clearance of dead cells in AT (Kosteli et al., 2010;Murano et al., 2008). While MCP-1 deficiency could regulate glucose tolerance independently of an effect on ATM proliferation, such as increased body weight or decreased accumulation of multiple immune cell types, our results indicate that proliferation may be a mechanism mediating the accumulation of ATM beneficial for glucose tolerance.

In summary, we show here that macrophage proliferation within VAT is a dynamic mechanism that increases with obesity and decreases during acute weight loss. Given the high proportion of macrophages (about 50%) that incorporate EdU over 80 hours, proliferation therefore likely contributes significantly, in addition to recruitment, to the accumulation of macrophages in the AT in obesity. At the molecular level, this study reveals MCP-1 as a potential stimulus for macrophage proliferation in obese AT.

EXPERIMENTAL PROCEDURES

Animals

8 to 12 week-old male wild-type C57BL/6J (WT) and B6.V-*Lepob*/*J* (*ob*/*ob*) mice were obtained from Jackson Laboratory and maintained on a 12-hour light/dark cycle. Animals were given free access to food and water. C57BL/6J wild-type mice were fed a high-fat diet (45% calories from lipids; D12451; Research Diets Inc.) for 7 weeks. All other mice were fed normal chow diet (Prolab 5P76 Isopro 3000, LabDiet). Six-week-old male MCP-1 knockout (KO) and wild-type (WT) mice on a C57BL/6J background were obtained from The Jackson Laboratory. Mice were fed a high-fat diet (60% calories from lipids; D12492; Research Diets Inc.) for 6 weeks. All procedures were performed in accordance with

protocols approved by the University of Massachusetts Medical School's Institutional Animal Care and Use Committee.

Isolation of macrophages from human and mouse adipose tissue

All protocols were approved by the University of Massachusetts Medical School Institutional Review Board. Human SAT was obtained from discarded tissue of 5 patients undergoing panniculectromy at UMASS Memorial Hospital. Adipose tissue SVF cells were prepared from collagenase-digested adipose tissue. Briefly, fat pads were digested with 2 mg/ml collagenase (Sigma) at 37°C for 45 minutes then filtered through 100 μm BD falcon cell strainers and spun at 300 *g* for 10 minutes at room temperature. The adipocyte layer and the supernatant were aspirated and the pelleted cells were collected as the SVF.

Liver and spleen cell isolation

Liver cells were isolated as previously described (Page and Garvey, 1979). Spleens were manually dissociated and the resultant cell suspension was centrifuged at 500 g.

Flow cytometry

For mice: cells were resuspended in PBS containing 1% BSA (FACS buffer) and Fc block (eBioscience) and allowed to block non-specific binding for 15 minutes at 4°C. Cells were then counted and incubated for an additional 20 minutes in the dark at 4°C with fluorophore-conjugated primary antibodies or isotype control antibodies. See supplementary methods for a complete list of antibodies used.

For the EdU experiments, cells were surface stained according to manufacturer's instructions. Following incubation with primary antibodies, cells were washed and fixed with fixation/permeabilization buffer (eBioscience) and then permeabilized with permeabilization buffer (eBioscience). EdU was chemically conjugated to Alexa 405 or Alexa 647 fluorophore according to the instructions of the manufacturer (Invitrogen). Sample data were acquired on a BD LSRII (BD Biosciences) and analyzed with FlowJo software (Tree Star).

Liposome Preparation and Depletion of Blood Monocytes

PBS and clodronate-loaded liposomes were prepared in a precisely scaled-down version of a method previously described (van Rooijen and van Kesteren-Hendrikx, 2003). *ob/ob* mice were injected i.v. with 200 μl of clodronate-loaded liposomes or equal volume of PBS-loaded liposomes every 16 hours. Small amounts of blood were taken at the end of several of the 16h periods and immediately before subsequent liposome injection to ensure monocyte depletion was continuous. Untreated mice did not receive any injections. 18 hours after the initial liposome injection, the mice were given drinking water containing 1mg/ml EdU. ATM content and EdU incorporation into ATMs were assessed by flow cytometric analysis 32h and 80h following exposure to EdU drinking water.

Explants and treatments

Pieces (1-2 mm^3) of VAT from *ob/ob* mice were treated with 10 μM EdU and 1 or 10 ng/ml of MCP-1 (Invitrogen). After 48 hours of treatment, SVF cells were isolated, counted and analyzed by flow cytometry.

Immunohistochemistry

Adipose tissue SVF cells and sections were stained and analyzed by fluorescent microscopy as previously described (Aouadi et al., 2013).

Isolation of RNA and Real Time PCR

RNA isolation was performed according to the Trizol Reagent Protocol (Invitrogen). cDNA was synthesized from 0.5-1 μg of total RNA using iScript cDNA Synthesis Kit (Bio-Rad) according to the manufacturer's instructions. For real time PCR, synthesized cDNA forward and reverse primers along with the iQ SYBR Green Supermix were run on the CFX96 Real-time PCR System (Bio-Rad). The ribosomal mRNA, 36B4 was used as an internal loading control.

Statistical analysis

All values are shown as means ± SEM. Student's *t*-test for two-tailed distributions with equal variances was used for comparison between two groups. Differences $p \leq 0.05$ were considered significant. Statistical analyses were performed with Graph Pad Prism 5. Please see Supplemental Methods and Supplemental Figures for detailed experimental procedures and additional data.

Supplementary Material

Refer to Web version on PubMed Central for supplementary material.

Acknowledgments

We thank Drs. S. Corvera, H. Kornfeld, S. Levitz, D. Greiner, J. Harris, and J. Virbasius and members of our laboratory group for excellent discussion of the data in this paper. We also appreciate the help of Richard Konz and the staff of Flow Cytometry and Morphology Cores in the University of Massachusetts. These studies were supported by grants to M.P.C. from the NIH (DK085753, AI046629), a grant from the International Research Alliance at Novo Nordisk Foundation Center for Metabolic Research, a grant from the JDRF (17-2009-546), and by Core Facilities in the University of Massachusetts Diabetes and Endocrinology Research Center also funded by the NIH (DK325220). J.L.C. is supported by the NIDDK of the NIH under NRSA postdoctoral fellowship F32DK098879.

REFERENCES

Allavena P, Bianchi G, Zhou D, van Damme J, Jilek P, Sozzani S, Mantovani A. Induction of natural killer cell migration by monocyte chemotactic protein-1, -2 and -3. Eur J Immunol. 1994; 24:3233–3236. [PubMed: 7805752]

Aouadi M, Tencerova M, Vangala P, Yawe JC, Nicoloro SM, Amano SU, Cohen JL, Czech MP. Gene silencing in adipose tissue macrophages regulates whole body metabolism in obese mice. Proc Natl Acad Sci U S A. 2013

Asterholm IW, McDonald J, Blanchard PG, Sinha M, Xiao Q, Mistry J, Rutkowski JM, Deshaies Y, Brekken RA, Scherer PE. Lack of "immunological fitness" during fasting in metabolically challenged animals. J Lipid Res. 2012; 53:1254–1267. [PubMed: 22504909]

Bjornson BH, Harvey JM, Rose L. Differential effect of hydrocortisone on eosinophil and neutrophil proliferation. J Clin Invest. 1985; 76:924–929. [PubMed: 3876356]

Bourlier V, Zakaroff-Girard A, Miranville A, De Barros S, Maumus M, Sengenes C, Galitzky J, Lafontan M, Karpe F, Frayn KN, et al. Remodeling phenotype of human subcutaneous adipose tissue macrophages. Circulation. 2008; 117:806–815. [PubMed: 18227385]

Feng B, Jiao P, Nie Y, Kim T, Jun D, van Rooijen N, Yang Z, Xu H. Clodronate liposomes improve metabolic profile and reduce visceral adipose macrophage content in diet-induced obese mice. PLoS One. 2011; 6:e24358. [PubMed: 21931688]

Guilherme A, Virbasius JV, Puri V, Czech MP. Adipocyte dysfunctions linking obesity to insulin resistance and type 2 diabetes. Nat Rev Mol Cell Biol. 2008; 9:367–377. [PubMed: 18401346]

Hashimoto D, Chow A, Noizat C, Teo P, Beasley MB, Leboeuf M, Becker CD, See P, Price J, Lucas D, et al. Tissue-Resident Macrophages Self-Maintain Locally throughout Adult Life with Minimal Contribution from Circulating Monocytes. Immunity. 2013; 38:792–804. [PubMed: 23601688]

Hinojosa AE, Garcia-Bueno B, Leza JC, Madrigal JL. CCL2/MCP-1 modulation of microglial activation and proliferation. J Neuroinflammation. 2011; 8:77. [PubMed: 21729288]

Inouye KE, Shi H, Howard JK, Daly CH, Lord GM, Rollins BJ, Flier JS. Absence of CC chemokine ligand 2 does not limit obesity-associated infiltration of macrophages into adipose tissue. Diabetes. 2007; 56:2242–2250. [PubMed: 17473219]

Jenkins SJ, Ruckerl D, Cook PC, Jones LH, Finkelman FD, van Rooijen N, MacDonald AS, Allen JE. Local macrophage proliferation, rather than recruitment from the blood, is a signature of TH2 inflammation. Science. 2011; 332:1284–1288. [PubMed: 21566158]

Jimenez F, Quinones MP, Martinez HG, Estrada CA, Clark K, Garavito E, Ibarra J, Melby PC, Ahuja SS. CCR2 plays a critical role in dendritic cell maturation: possible role of CCL2 and NF-kappa B. J Immunol. 2010; 184:5571–5581. [PubMed: 20404272]

Kanda H, Tateya S, Tamori Y, Kotani K, Hiasa K, Kitazawa R, Kitazawa S, Miyachi H, Maeda S, Egashira K, et al. MCP-1 contributes to macrophage infiltration into adipose tissue, insulin resistance, and hepatic steatosis in obesity. J Clin Invest. 2006; 116:1494–1505. [PubMed: 16691291]

Kosteli A, Sugaru E, Haemmerle G, Martin JF, Lei J, Zechner R, Ferrante AW Jr. Weight loss and lipolysis promote a dynamic immune response in murine adipose tissue. J Clin Invest. 2010; 120:3466–3479. [PubMed: 20877011]

Lee YH, Petkova AP, Mottillo EP, Granneman JG. In vivo identification of bipotential adipocyte progenitors recruited by beta3-adrenoceptor activation and high-fat feeding. Cell Metab. 2012; 15:480–491. [PubMed: 22482730]

Lumeng CN, DelProposto JB, Westcott DJ, Saltiel AR. Phenotypic switching of adipose tissue macrophages with obesity is generated by spatiotemporal differences in macrophage subtypes. Diabetes. 2008; 57:3239–3246. [PubMed: 18829989]

Mayi TH, Daoudi M, Derudas B, Gross B, Bories G, Wouters K, Brozek J, Caiazzo R, Raverdi V, Pigeyre M, et al. Human adipose tissue macrophages display activation of cancer-related pathways. J Biol Chem. 2012; 287:21904–21913. [PubMed: 22511784]

Morris DL, Cho KW, Delproposto JL, Oatmen KE, Geletka LM, Martinez-Santibanez G, Singer K, Lumeng CN. Adipose tissue macrophages function as antigen-presenting cells and regulate adipose tissue CD4+ T cells in mice. Diabetes. 2013b; 62:2762–2772. [PubMed: 23493569]

Murano I, Barbatelli G, Parisani V, Latini C, Muzzonigro G, Castellucci M, Cinti S. Dead adipocytes, detected as crown-like structures, are prevalent in visceral fat depots of genetically obese mice. J Lipid Res. 2008; 49:1562–1568. [PubMed: 18390487]

Nomiyama T, Perez-Tilve D, Ogawa D, Gizard F, Zhao Y, Heywood EB, Jones KL, Kawamori R, Cassis LA, Tschop MH, et al. Osteopontin mediates obesity-induced adipose tissue macrophage infiltration and insulin resistance in mice. J Clin Invest. 2007; 117:2877–2888. [PubMed: 17823662]

Oh DY, Morinaga H, Talukdar S, Bae EJ, Olefsky JM. Increased Macrophage Migration Into Adipose Tissue in Obese Mice. Diabetes. 2011

Olefsky JM, Glass CK. Macrophages, inflammation, and insulin resistance. Annu Rev Physiol. 2010; 72:219–246. [PubMed: 20148674]

Page DT, Garvey JS. Isolation and characterization of hepatocytes and Kupffer cells. J Immunol Methods. 1979; 27:159–173. [PubMed: 458170]

Sager HB, Middendorff R, Rauche K, Weil J, Lieb W, Schunkert H, Ito WD. Temporal patterns of blood flow and nitric oxide synthase expression affect macrophage accumulation and proliferation during collateral growth. J Angiogenes Res. 2010; 2:18. [PubMed: 20843382]

Scholzen T, Gerdes J. The Ki-67 protein: from the known and the unknown. J Cell Physiol. 2000; 182:311–322. [PubMed: 10653597]

Talukdar S, Oh da Y, Bandyopadhyay G, Li D, Xu J, McNelis J, Lu M, Li P, Yan Q, Zhu Y, et al. Neutrophils mediate insulin resistance in mice fed a high-fat diet through secreted elastase. Nat Med. 2012; 18:1407–1412. [PubMed: 22863787]

van Rooijen N, van Kesteren-Hendrikx E. “In vivo” depletion of macrophages by liposome-mediated “suicide”. Methods Enzymol. 2003; 373:3–16. [PubMed: 14714393]

Weisberg SP, Hunter D, Huber R, Lemieux J, Slaymaker S, Vaddi K, Charo I, Leibel RL, Ferrante AW Jr. CCR2 modulates inflammatory and metabolic effects of high-fat feeding. J Clin Invest. 2006; 116:115–124. [PubMed: 16341265]

Weisberg SP, McCann D, Desai M, Rosenbaum M, Leibel RL, Ferrante AW Jr. Obesity is associated with macrophage accumulation in adipose tissue. J Clin Invest. 2003; 112:1796–1808. [PubMed: 14679176]

Wu D, Molofsky AB, Liang HE, Ricardo-Gonzalez RR, Jouihan HA, Bando JK, Chawla A, Locksley RM. Eosinophils sustain adipose alternatively activated macrophages associated with glucose homeostasis. Science. 2011; 332:243–247. [PubMed: 21436399]

Xu H, Barnes GT, Yang Q, Tan G, Yang D, Chou CJ, Sole J, Nichols A, Ross JS, Tartaglia LA, et al. Chronic inflammation in fat plays a crucial role in the development of obesity-related insulin resistance. J Clin Invest. 2003; 112:1821–1830. [PubMed: 14679177]

Yang JP, Renzi PM. Interleukin-2 and lymphocyte-induced eosinophil proliferation and survival in asthmatic patients. J Allergy Clin Immunol. 1993; 91:792–801. [PubMed: 8454801]

Highlights

- Macrophages undergo cell division locally within adipose tissue in mice
- Obesity increases the proliferation of macrophages in adipose but not other tissues
- Macrophage proliferation occurs independently of monocyte recruitment
- MCP-1 stimulates adipose tissue macrophage cell division

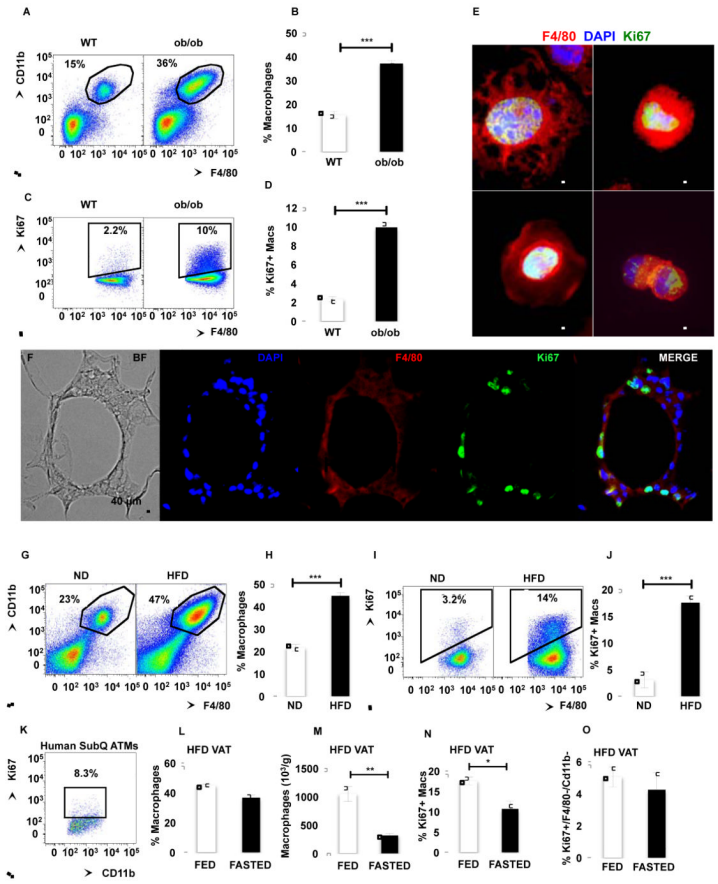

Figure 1. Adipose tissue macrophages express the cell division marker Ki67

See also Figure S1. SVF from VAT of WT and *ob*/*ob* mice was isolated and analyzed by flow cytometry. (**A**) Representative flow cytometry dot plots. (**B**) Percentage of macrophages in SVF. (**C**) Representative flow cytometry dot plots of ATMs stained with Ki67. (**D**) Percentage of macrophages expressing Ki67. n=30-31 from 6 independent experiments. (**E**) Microscopy of plated SVF stained with antibodies against F4/80 (red) and Ki67 (green). Nuclei were stained with DAPI (Blue). 63x magnification images. Scale bar = 5 μm. (**F**) VAT of *ob*/*ob* mice containing CLS stained with antibodies against F4/80 (red) and Ki67 (green). Nuclei were stained with DAPI (Blue). 20x magnification images. Scale bar = 40 μm. (**G**) SVF from VAT of mice fed a ND or HFD for 7 weeks was isolated and analyzed by flow cytometry. Representative flow cytometry dot plots. (**H**) Mean percentage of macrophages in SVF. (**I**) Representative flow cytometry dot plots of ATMs stained with Ki67. (**J**) Percentage of macrophages expressing Ki67. n=30-31 from 6 independent experiments. (**K**) Representative dot plot of SVF from human SAT stained with Ki67. (**L**) Percentage of macrophages in SVF from VAT of mice fed a HFD for 7 weeks and fasted for 24 hours. n=8-18. (**M**) Number of macrophages in SVF from VAT of mice fed a HFD and fasted for 24 hours. n=5. (**N**) Percentage of macrophages expressing Ki67 in fasted mice. n=8-18. (**O**) Percentage of non-macrophages (CD11b−/F4/80−) expressing Ki67. n=8-18. All graphs are expressed as mean ± s.e.m. Statistical significance was determined by Student's t-test. ***p<0.001; **p<0.01; *p<0.05 .

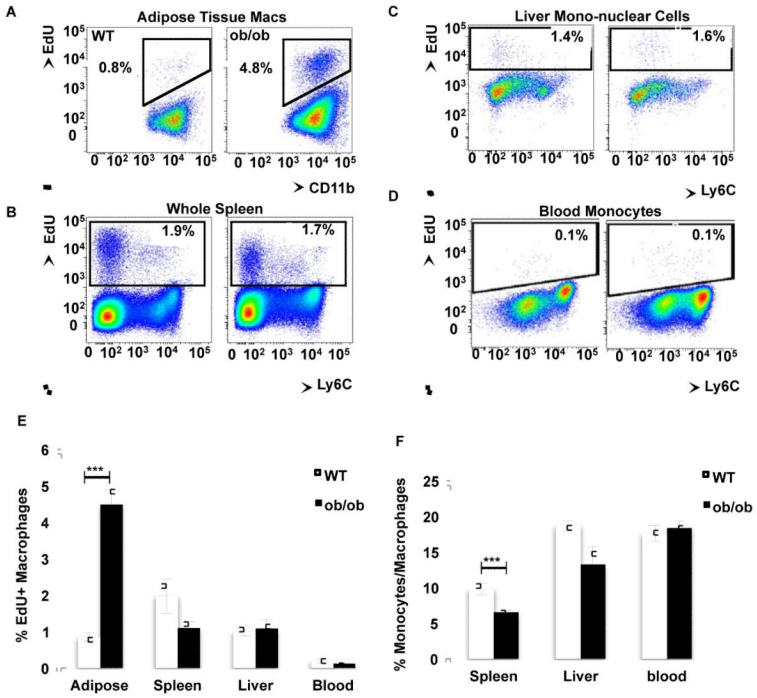

Figure 2. Obesity increases macrophage proliferation specifically in adipose tissue

See also Figure S2. WT and *ob/ob* mice were i.p. injected with EdU and (**A**) AT, (**B**) spleen, (**C**) liver and (**D**) blood were collected and digested 3 hours after treatment. All cells were stained and analyzed by flow cytometry. Representative dot plots depict the EdU incorporation into all cells of the respective tissues or blood monocytes. (**E**) Mean percentage of EdU incorporation rate of the macrophages of each tissue ± s.e.m. (**F**) Percentage of macrophages in each tissue. n= 14-15 from 3 independent experiments for AT and blood, and n=9-10 from 2 independent experiments for spleen and liver. Statistical significance was determined by Student's t-test. ***p<0.001.

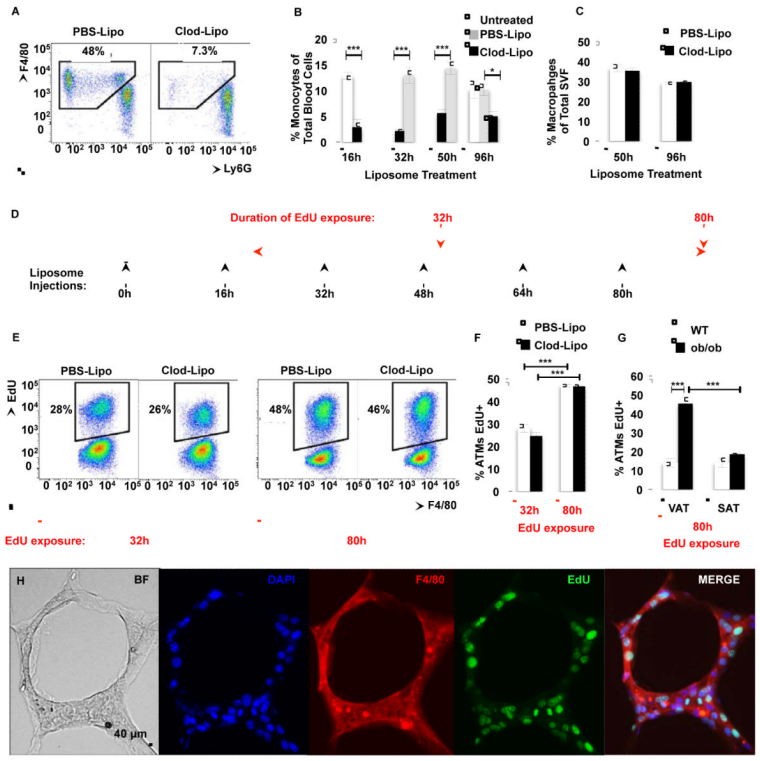

Figure 3. Adipose tissue macrophages proliferate independently of monocyte recruitment

See also Figure S3. *ob*/*ob* mice were i.v. injected with either PBS-Lipo or Clod-Lipo every 16 hours. (**A**) Example flow cytometry dot-plots of $CD11b^+$ blood cells show depletion of monocytes, and (**B**) the quantitation of blood monocytes expressed as a percentage of total blood cells. n=10 for 16h-48h of liposome treatment and n=4-5 for the 96h time point. (**C**) Macrophage content in the AT of PBS-liposome and clodronate-liposome-treated *ob*/*ob* mice; n=5 mice per group. 18 hours after initial injection, the mice were given drinking water containing EdU. (**D**) Diagram representing experimental design of treatment. (**E**) Representative flow cytograms and (**F**) quantification of EdU incorporation into ATMs during 32h and 80h of exposure to EdU drinking water in PBSLipo-treated and monocyte-depleted Clod-Lipo-treated *ob*/*ob* mice. (**G**) Quantification of EdU incorporation into ATMs during 80h of exposure to EdU drinking water in VAT and SAT in lean WT and *ob/ob* obese mice. n= 5 mice per group. All graphs are expressed as mean ± s.e.m. Statistical significance was determined by Student's t-test or two-way ANOVA followed by Tukey post-test. ***p<0.001; **p<0.01; *p<0.05. (**H**) VAT of *ob*/*ob* mice containing CLS stained with antibodies against F4/80 (red) and EdU (green). Nuclei were stained with DAPI (Blue). 20x magnification images. Scale bar = 40 μm.

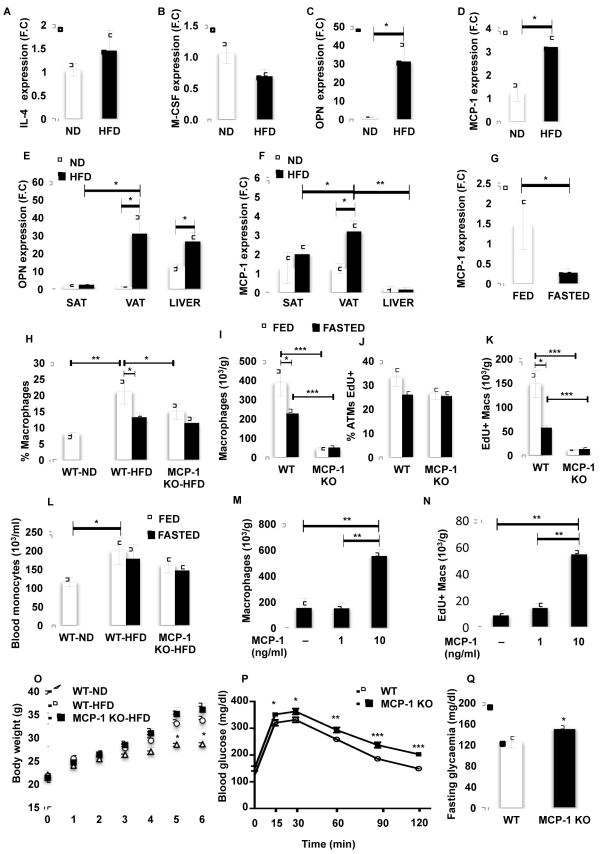

Figure 4. MCP-1 is required for optimal adipose tissue macrophage proliferation

See also Figure S4. VAT was isolated from mice fed a ND or HFD for 7 weeks. (**A**) IL-4, (**B**) M-CSF, (**C**) OPN and (**D**) MCP-1 expression was measured by RT-PCR. n=5. (**E**) Expression of OPN and (**F**) MCP-1 in SAT, VAT and liver from mice fed a ND or HFD for 7 weeks. n=5. (**G**) Expression of MCP-1 in VAT of mice fed a HFD for 7 weeks and fasted for 24 hours. (**H**) Percentage and (**I**) number of macrophages in SVF from VAT of MCP-1 KO and WT mice fed a HFD for 6 weeks and fasted for 18 hours. n=5. (**J**) Percentage and (**K**) number of EdU^+ macrophages in AT of MCP-1 KO and WT mice. (**L**) Number of blood monocytes in MCP-1 KO and WT mice. Explants from VAT of 5 *ob/ob* mice were treated with 1 and 10 ng/ml of MCP-1 in presence of 10 μM of EdU for 48 hours. Graph represents the number of (**M**) macrophages and (**N**) EdU^+ macrophages in explants. (**O**) Body weight of MCP-1 KO and WT mice fed a HFD for 6 weeks. (**P**) GTT and (**Q**) fasting glycaemia. All graphs are expressed as mean ± s.e.m. Statistical significance was determined by Student's t-test or two-way ANOVA followed by Tukey post-test. ***p<0.001; **p<0.01; *p<0.05.